2015년 2월
석사학위논문

무인항공기를 위한 화학수소화물 기반 고분자 전해질 막 연료전지 시스템의 설계 및 성능평가

조선대학교 대학원

항공우주공학과

김 진 철

무인항공기를 위한 화학수소화물 기반 고분자 전해질 막 연료전지 시스템의 설계 및 성능평가

Design and performance evaluation of PEMFC system based on chemical hydride for UAV applications

2015년 2월 25일

조선대학교 대학원

항공우주공학과

김 진 철

무인항공기를 위한 화학수소화물 기반 고분자 전해질 막 연료전지 시스템의 설계 및 성능평가

지도교수 김 태 규

이 논문을 공학 석사학위신청 논문으로 제출함

2014 년 11 월

조선대학교 대학원

항공우주공학과

김 진 철

김진철의 석사학위 논문을 인준함

위원장 한밭대학교 교수	이 종 광 (인)
위 원 조선대학교 교수	김 태 규 (인)
위 원 조선대학교 교수	오 현 웅 (인)

2014 년 11 월

조 선 대 학 교 대 학 원

Table of contents

LIST OF FIGURES

LIST OF TABLES

NOMENCLATURE

Abbreviations

UAV	Unmanned Aerial Vehicle
FC	Fuel Cell
MCFC	Molten Carbon Fuel Cell
SOFC	Solid Oxide Fuel Cell
AFC	Alkaline Fuel Cell
PAFC	Phosphoric Acid Fuel Cell
PEMFC	Polymer Electrode Membrane Fuel Cell
GDL	Gas Diffusion Layer
MOSFET	Metal Oxide Semiconductor Field Effect Transistor
MEA	Membrane Electrode Assembly
MFM	Mass Flow Meter
DAQ	Data Acquisition
STP	Standard conditions for Temperature and Pressure
MOF	Metal-Organic Frameworks
BOP	Balance Of Plant

Electricity

W	Watt
A	Current
V	Voltage
Ω	Ohm
V_{DROP}	Voltage Drop

Unit

kPa	Kilopascal
s	Second
ms	millisecond
m^3/min	Cubic meter per minute
L/min	Liter per minute
MJ/kg	Megajoule per kilogram
MJ/L	Megajoule per litter
RPM	Revolutions per minute

Chemistry

H_2	Hydrogen
CO	Carbon monoxide
CO_2	Carbon dioxide
$NaBH_4$	Sodium borohydride
$ZnBH_4$	Zinc borohydride
$CaBH_4$	Calcium borohydride
$LiAlH_4$	Lithium aluminium hydride
$NaBH(OCH_3)_3$	Sodium trimethoxy borohydride
$NaBO_2$	Sodium metaborate
Ru	Ruthenium
Rh	Rhodium
Pt	Platinum
Ni	Nickel
Co	Cobalt
Cu	Copper
Co-B	Cobalt boride

ABSTRACT

Design and performance evaluation of PEMFC system based on chemical hydride for UAV applications

by Kim, Jincheol

Advisor : Prof. Kim, Taegyu, Ph. D.

Department of Aerospace Engineering,

Graduate School of Chosun University

본 논문에서는 무인항공기를 위한 연료전지 시스템을 설계하였다. 대부분의 무인시스템은 2차 전지를 기반으로 제작되어있는데, 이들 2차 전지를 전력원으로 사용 할 경우 낮은 에너지 밀도로 인해 작동시간이 제한된다. 해서 본 논문에서는 에너지 밀도가 높은 고분자 전해질 막 연료전지를 통해서 상용의 무인항공기 시스템보다 높은 작동시간을 가지는 시스템을 설계하였다. 특히 본 시스템에서는 고분자 전해질 막 연료전지를 활용하였다. PEMFC는 작동온도가 낮고 전해질이 고체이며 소형화하기에 용이하기 때문에 본 시스템에 적합하다고 판단하였다.

본 시스템을 활용하기 위해 두가지를 실험하였는데, 먼저 과전류 제어기를 통해 고분자 전해질 막 연료전지 (Polymer electrolyte membrane fuel cell; PEMFC) 내부를 가습하는 연구를 수행하였다. 대체적으로 연료전지는 별도의 외부 가습장치를 통해서 연료전지 내부가 건조해지는 것을 방지한다. 게다가 무인항공기에서는 습도조절이 더욱 더 중요한데, 이는 비행고도에 따른 비등점의 변화로 인해 연료전지 내부가 쉽게 건조해질 수 있기 때문이다.

연료전지 내부 전해질 막의 가습을 위해서 과전류를 발생시키고 연료전지의 출력을

향상시키는 것을 목표로 다음과 같은 실험을 수행하였다. 과전류 제어를 위한 회로를 포함하여 연료전지 제어기가 제작되었고, 추가적으로 배터리를 연결하여 과전류 제어를 할 때 발생하는 전압강하를 보조하는 역할을 하게 된다.

과전류 발생기에서 알고리즘 수정을 통해 과전류 발생 주기와 간격을 조정하며 그에 따른 연료전지 성능변화를 측정하였다. 실험결과로 과전류 발생 제어를 통해서 출력이 최대 16% 향상되는 것을 확인하였다.

두 번째로 무인 시스템을 위한 화학 수소화물 기반의 소형 연료전지 시스템을 제작하였다. 기본적으로 연료전지는 수소를 연료로 하여 전력을 생산한다. 이를 위한 다양한 수소공급방식이 있으나 그 대부분이 시스템의 복잡성과 무게가 증가하는 등 소형화에 부적합하다고 판단하였다. 따라서 화학 수소화물을 기반으로 한 수소 저장방식이 채택되었고, 그 중에서 가격이 저렴하고 수소저장밀도가 10.8%인 수소화 붕소나트륨을 선정하였다.

이러한 화학 수소화물은 기본적으로 가수분해반응을 통해서 수소를 생성하게 된다. 하지만 가수분해반응 만으로는 안정적인 전력생산을 위한 수소유량공급에 부적합하다고 판단하여 Co-B/Ni촉매를 활용하였다. 안정작인 수소유량공급을 위해 일체형 수소발생기를 제작하였다. 그 외에도 펌프와 밸브를 통해서 연료를 공급하고 $NaBO_2$를 배출하게 된다.

본 시스템을 통해서 수소 발생기의 성능을 검증하고 나아가 100W급 연료전지를 통해서 수소 공급 성능 및 수소 순도를 평가하였다.

I. Introduction

A. Active humidification of PEMFC using short circuit control

Unmanned aerial vehicles (UAVs) have been used for meeting civilian demands and military purposes in diverse fields, particularly for reconnaissance and surveillance. For these missions, high endurance of UAVs for maximizing their capability is preferred to attributes such as quiet operations or maneuverability. However, conventional internal combustion engines running on gasoline and diesel are still employed as the main source for powering the UAVs. Although the internal combustion engine can generate power through combustion, the exhaust emissions produced during the process cause serious environmental problems. In addition, fossil fuels (which are the energy sources for internal combustion engines) are on the brink of exhaustion, necessitating a new, next-generation power source for UAVs. Recently, the fuel cell (FC) has gained attention as a new power source because it possesses higher energy density than fossil fuels. Moreover, the FC is ecofriendly because its byproducts are only water and heat.

Various types of FCs are available, including molten carbon FC, solid oxide FC, alkaline FC, phosphoric acid FC, and polymer electrolyte membrane FC (PEMFC). Among these, the PEMFC is suitable for UAVs because of the following advantages: 1) high loading capability due to relatively lighter weight, and ease of miniaturization; 2) low operating temperature at which ion conductivity is adequate to generate high power; 3) use of solid-state electrolyte, thereby eliminating sloshing problems due to vibrations during flight; and 4) higher thermal efficiency compared to other FCs. Owing to these advantages, PEMFCs are being developed as portable power sources, particularly for UAVs in aeronautical applications [1]. Many PEMFC-powered UAVs have been developed worldwide, such as the *Ion*

Tiger by the Naval Research Laboratory [2], *PUMA* by the Air Force Research Laboratory [3], *Phantom Eye* by Boeing [4] in the United States, *Hyfish* by the German Air & Space Center [5] in Germany, *FAUCON H2* by EnergyOr Technologies [6] in Canada, *BirdEye-650* by Aerospace Industries [7] in Israel, and the Korea Aerospace Research Institute in Korea. Moreover, the FC system for UAVs has been widely studied at universities such as the Washington State University [8] in the United States, National Cheng Kung University [9] in Taiwan, Nanyang Technological University [10] in Singapore, Korea Advanced Institute of Science and Technology, and Chosun University in Korea [11 - 12].

The FC is a simple device in which hydrogen is reduced into an ion and two electrons, and as the hydrogen ion passes through an electrolyte and combines with oxygen, it generates electricity along with water and heat. In this process, humidity control in the polymer electrolyte membrane is very important because water plays the role of an ion-conducting carrier [13]. When the membrane has the correct water content, the power output of the FC is maximized. High content (indicating high humidity) causes water flooding, which blocks the pores of the gas diffusion layer (GDL) and inhibits the passage of oxygen. When the FC is dry (indicating low humidity), the electric resistance in the membrane increases, causing the voltage to drop with increase in current [14 - 18]. Therefore, FC performance depends strongly on its internal humidity and generally deteriorates when the latter is much higher or lower than desired.

Owing to this dependence, a typical FC system uses an external humidifier to control its internal humidity. However, this makes it heavy and bulky and hence unsuitable for UAV applications. In particular, the FC system should be of small size and less weight for small UAVs because their payload capacity is limited. Therefore, eliminating the external humidifier in the FC releases additional payload capacity in the UAV for other missions.

In the present study, the short circuit technique was used to control the internal humidity of the FC. Momentary short-circuiting generated overcurrent in the FC, causing hydrogen to react considerably with oxygen to generate water, thus humidifying the electrolyte membrane. A fuel-cell short circuit controller was developed and the humidification performance was examined for different short circuit intervals and durations. In addition, the performance characteristics of the FC were evaluated with and without the short circuit controller.

Table. 1 Classification of the FC according to electrolyte

	PEMFC	AFC	PAFC	MCFC	SOFC
Electrolyte	Hydrated Polymeric Ion Exchange Membranes	Mobilized or Immobilized Potassium Hydroxide in asbestos matrix	Immobilized Liquid Phosphoric Acid in SiC	Immobilized Liquid Molten Carbonate in $LiAlO_2$	Perovskites (Ceramics)
Electrodes	Carbon	Transition metals	Carbon	Nickel and Nickel Oxide	Perovskite and perovskite / metal cermet
Catalyst	Platinum	Platinum	Platinum	Electrode material	Electrode material
Interconnect	Carbon or metal	Metal	Graphite	Stainless steel or Nickel	Nickel ceramic or steel
Operating Temperature	40-80℃	65-220℃	205℃	650℃	600-1000℃
Charge Carrier	H^+	OH^-	H^+	$CO3^{2-}$	O^{2-}
External Reformer for Hydrocaron Fuels	Yes	Yes	Yes	No. For some fuels	No. For some fuels and cell designs
External shift conversion of CO to hydrogen	Yes. Plus purification to remove trace CO	Yes. Plus purification to remove trace CO and CO_2	Yes	No	No
Prime Cell Components	Carbon-based	Carbon-based	Graphite-based	Stainless-based	Ceramic
Product Water Management	Evaporative	Evaporative	Evaporative	Gaseous product	Gaseous product
Product Heat Management	Process gas + Liquid cooling medium	Process gas + Electrolyte circulation	Process gas + Liquid cooling medium or steam generation	Internal reforming + Process gas	Internal reforming + Process gas

B. Chemical hydride hydrogen storage for compact PEMFC system

Up to now, a polymer electrolyte membrane fuel cell (PEMFC) has been adopted for the UAVs but the hydrogen storage density was too low to realize the high energy density of the fuel cell system using the hydrogen as a fuel. Basically, hydrogen has gravimetric energy density (120 MJ/kg) three times higher than gasoline (44 MJ/kg). However, the volumetric energy density (0.01 MJ/L at STP) is much lower than gasoline (32 MJ/L). Thus, the high-density hydrogen storage is important for determining the energy density of PEMFC systems for UAV applications. In addition, the hydrogen storage method would have high storability and good mobility [19 - 21].

Currently-available hydrogen storage method includes compressed hydrogen, liquid and cryo-compressed hydrogen, sorbents, metal hydrides, metal-organic frameworks (MOF), and carbon-based material [20, 28, 29, 32 - 36]. However, conventional hydrogen storage methods are still problematic because the hydrogen storage density is low and the device is bulky and complex. Recently, it is reported that MOF and carbon-based hydrogen storages have realized the desirable hydrogen storage density but they require high manufacturing technologies [19]. As a result, these hydrogen storage methods suffer from technical difficulties in manufacture, the increased expense for the maintenance, and problems that make the system bulky and heavy. Thus, we need an alternative method for hydrogen storage to complement the above problems. Recently, chemical hydrides have attracted a great interest as an alternative of hydrogen storage for UAV applications.

In the present study, a fuel cell system using the hydrogen storage based on the chemical hydride was developed for portable applications. There are many chemical hydrides available including $NaBH_4$, $ZnBH_4$, $CaBH_4$, $LiAlH_4$, $NaBH(OCH_3)_3$ and so on. Chemical hydrides are stored stably as it is at the atmospheric condition, while hydrogen can be extracted readily by chemical decomposition when needed. The chemical hydride has advantageous to portable fuel cells because of its high hydrogen capacity and possibility of hydrogen storage/supply at the atmospheric condition. Particularly, chemical hydrides can be stored and carried in the state of an alkali solution, and hydrogen can be extracted from the solution as well as directly in the solid state [23]. The chemical hydrides mainly consist of alanate hydrides, alkali metal hydrides, and metal hydro-borates [22]. Among them, sodium borohydride ($NaBH_4$) metal that is a kind of hydro-borates has been widely studied as the chemical hydride-based hydrogen storage because it is cheaper and the energy density per unit volume/mass is higher than other types of chemical hydrides [19, 22, 24 - 28]. Thus, the $NaBH_4$ was selected as a hydrogen source for the PEMFC system in the present study.

Hydrogen can be generated by the hydrolysis reaction of $NaBH_4$ The hydrolysis reaction should be accelerated and stabilized to supply hydrogen stably and continuously. There are two ways that have been widely used; one is to use a catalyst and the other is to control pH value by acids [19, 21, 25]. When acids are used, the hydrogen generation is reliable but the hydrogen generation rate was not controllable without control mechanisms and the acid is difficult to handle and store. Considering the aspect of safety, the catalytic hydrolysis of $NaBH_4$ was selected for portable applications. Up to now, noble catalysts such as Ru, Rh, and Pt, and non-noble catalysts such as Ni, Co, and Cu have been studied for the catalytic hydrolysis of $NaBH_4$. In the present study, Co-B/Ni foam was used as a catalyst because of its relatively low cost and high performance [22, 24, 25, 28]. However, there are still problem in the catalytic hydrolysis. First, the catalyst can be deactivated by the deposition of $NaBO_2$ that is a byproduct of the hydrolysis of $NaBH_4$ [38 - 40]. In addition, the device for generating pure hydrogen from $NaBH_4$ should equip the catalytic reactor, hydrogen separator, and $NaBO_2$ chamber, which are very complex and makes the system bulky and heavy [29, 31, 40].

In the present study, the all-in-one reactor was designed in which the catalytic reactor, hydrogen separator, and $NaBO_2$ chamber were combined in a single space. In addition, all of balance-of-plant (BOP) such as a pump, valve, cooling fan, and controller were integrated to develop the complete hydrogen generator. The developed hydrogen generator was connected to a 100 W PEMFC stack and the performance was evaluated according to the electronic load.

II. Experiments

A. FC control system

The schematic of the FC controller is presented in Fig. 1. It consists of (i) DC/DC convertor to regulate the voltage to the microprocessor and sensors, (ii) current sensor to measure the FC stack current, (iii) power-metal oxide semiconductor field effect transistor (power-MOSFET) (IRFP4110PbF) to short circuit the FC stack, (iv) transistors to operate the purging valve and cooling fans, and (v) 128-bit microprocessor (Atmega 128) to control the components as programmed. When the FC stack is short-circuited, the power should be compensated to provide a stable output to the electric load. To achieve this, the FC stack was connected parallel with an auxiliary lithium-polymer battery (24 V, 3-cells) in this experiment. Furthermore, the battery and FC stack simultaneously supplied power when a sudden load was applied.

A control algorithm was programmed to control the components of the FC stack including the cooling fans and anode purging valve, which were operated using a pulse width modulation signal at the interval and for the duration previously determined. The FC controller was programmed to direct the short circuit current to the FC stack at various intervals (periods) and for different durations. Figure 2 shows the periods and durations of short circuit in the FC stack. Short circuit period refers to the frequency (interval) of short-circuiting or the time between the n and n+1 short signals in a periodic short circuit operation. Short circuit duration refers to the time for which the FC stack is short-circuited. In this study, short circuit periods of 2, 10, and 60 s were used and the short circuit duration was fixed at 100 ms because long short circuit time causes excessive water flooding at the cathode and damages the membrane electrode assembly (MEA) of the FC stack.

The performance of the FC can be altered by varying the short circuit period and duration. When the FC is short-circuited, the voltage drops suddenly, as shown in Fig. 2. However, in the present study, a hybrid system of the FC and battery was used to avoid a voltage drop below the battery voltage (~24 V). Therefore, a stable power output could be provided to the load (such as an electric motor) by maintaining a very short (~100 ms) duration of short circuit and ensuring that the voltage was always higher than the motor's rated voltage even when the FC was short-circuited.

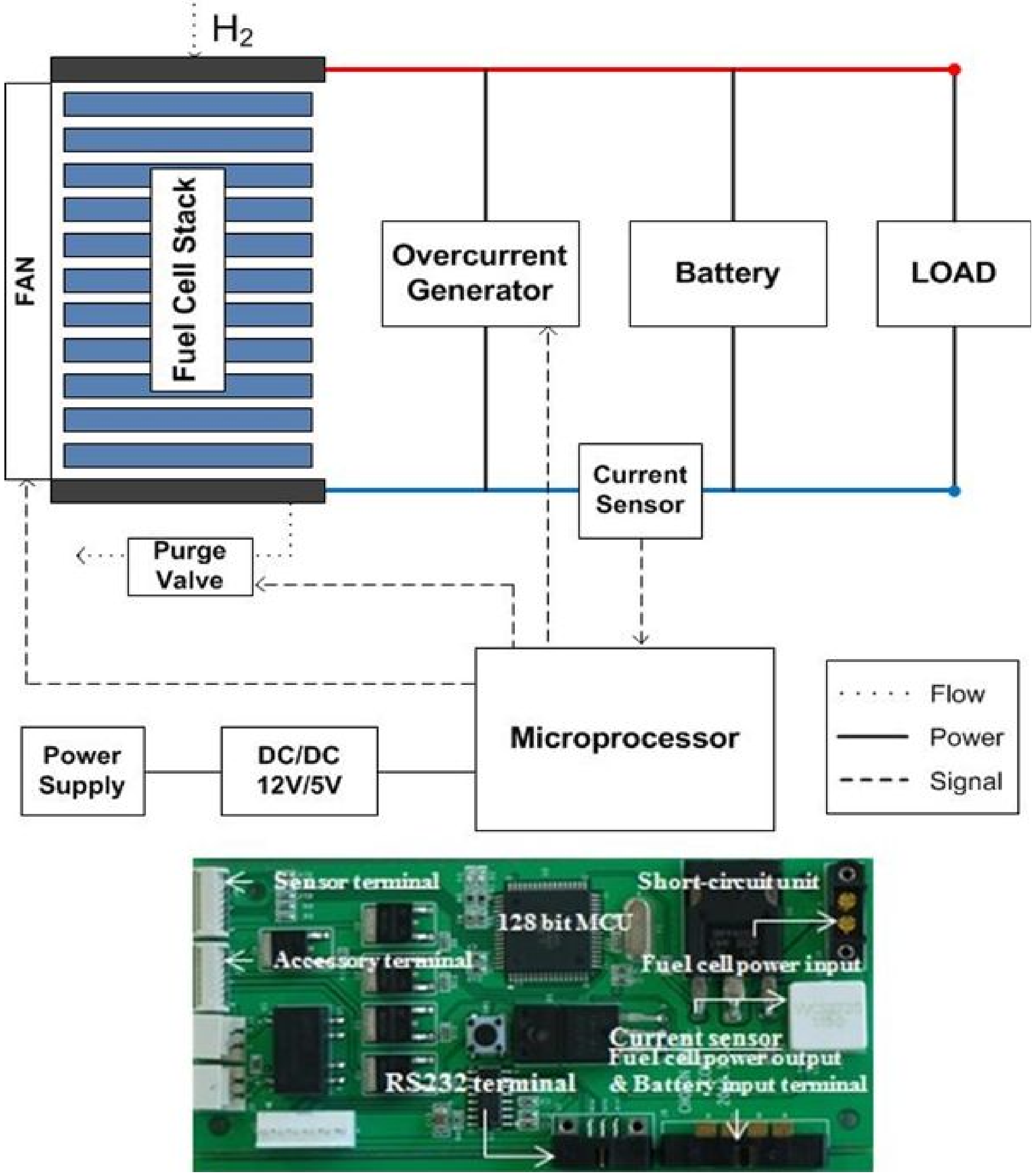

Fig. 1 Schematic of FC controller

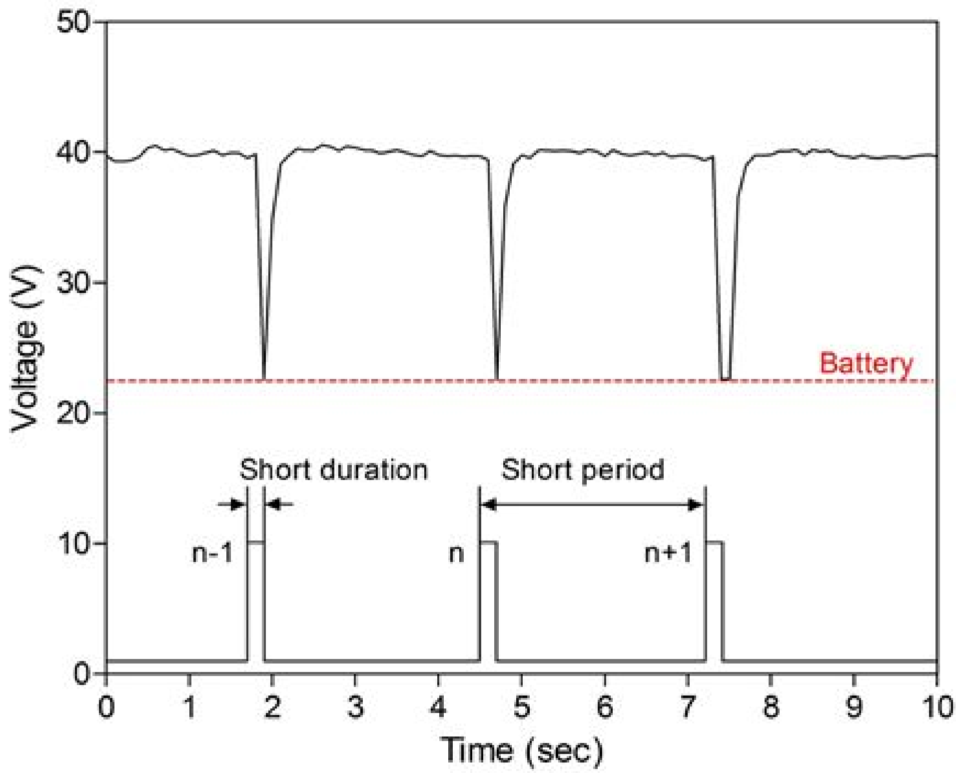

Fig. 2 Period and duration of short circuit in FC stack

B. Compact PEMFC system design

The developed compact PEMFC system using the hydrogen generator based on the $NaBH_4$ chemical hydride is shown in Fig. 3. The system consists of three parts; the PEMFC stack, hydrogen generator, and $NaBH_4$ fuel tank. First, 100 W lightweight PEMFC stack was used. Particularly, bipolar plates were manufactured by metal forming so that the weight and volume of the stack could be reduced considerably. Next, the hydrogen generator has an all-in-one reactor in which the $NaBH_4$ hydrolysis takes place and the generated hydrogen is pressurized temporally. The exploded view of the all-in-one reactor is shown in Fig. 4. The reactor consists of three parts; the catalytic reactor, byproduct separator, and hydrogen chamber. The Co-B/Ni foam catalyst was packed in the catalytic reactor as shown in Fig. 5. The Co-B is an active material for the $NaBH_4$ hydrolysis and the Ni foam is the support of Co-B. The catalyst was prepared by electroless plating. The foam catalyst was very easy to be shaped and the replacement was very simple.

The $NaBH_4$ solution was supplied into the catalytic reactor by the pump and then the hydrolysis reaction took place on the catalyst, immediately generating hydrogen. The generated hydrogen was stored temporally in the hydrogen chamber maintaining the pressure of 5 bar. Hydrogen was supplied to the fuel cell after the pressure was adjusted to 0.6 bar through the pressure regulator. The $NaBO_2$ was collected in the byproduct separator and discharged through the valve into the outside according to the amount of $NaBH_4$ supplied by the pump. The cooling fins were attached on the reactor to cool the heat of reaction of the $NaBH_4$ hydrolysis that is exothermic. Cooling fans were installed on the case of the fuel cell system to maintain the constant temperature in the reactor. The $NaBH_4$ solution was stored in the fuel tank that is easy to be detachable from the system, which facilitated the safe storage and porterage.

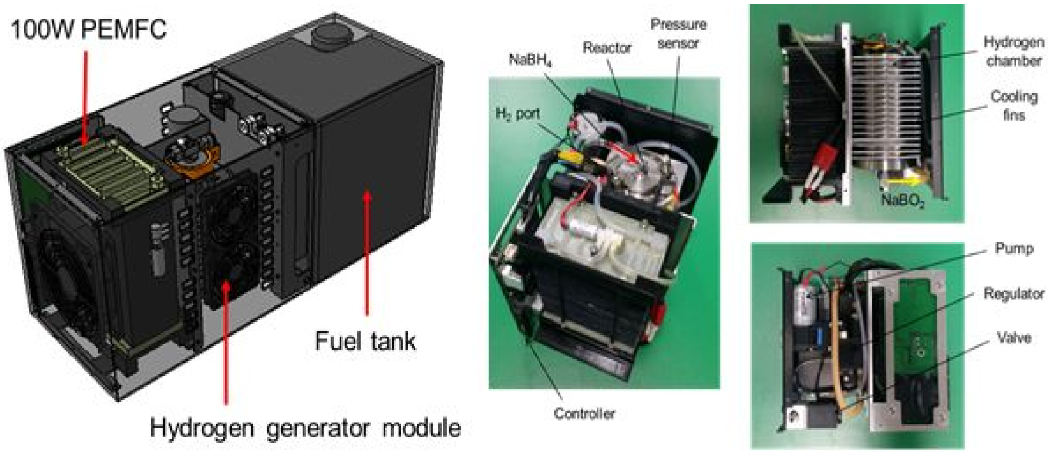

Fig. 3 Developed compact PEMFC system using the hydrogen generator based on the $NaBH_4$ chemical hydride

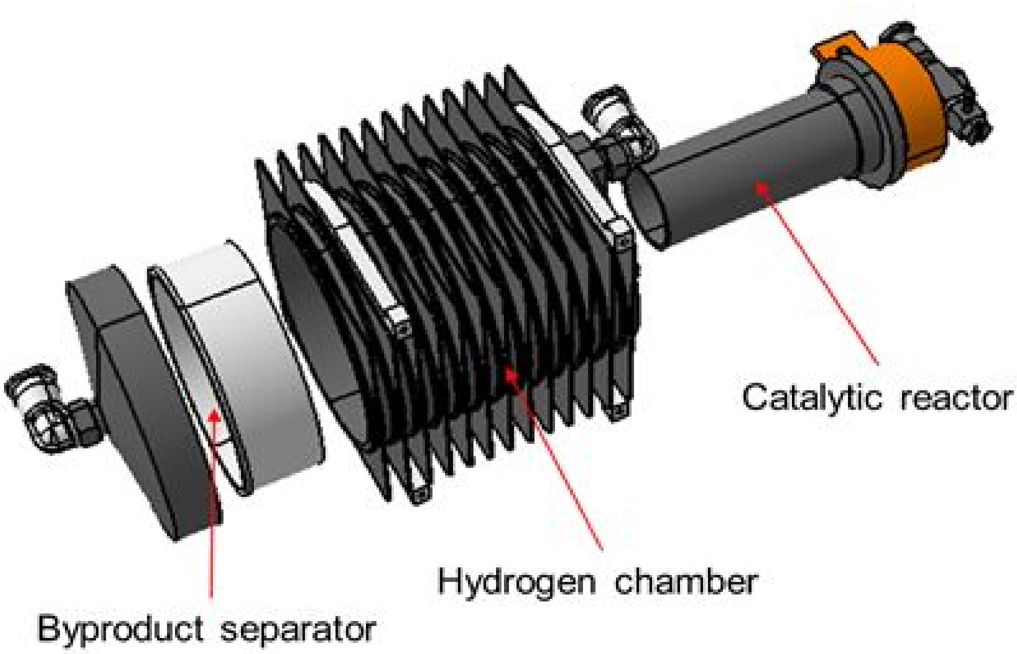

Fig. 4 Schematic of the all-in-one reactor in which the $NaBH_4$ hydrolysis takes place and the generated hydrogen is pressurized temporally

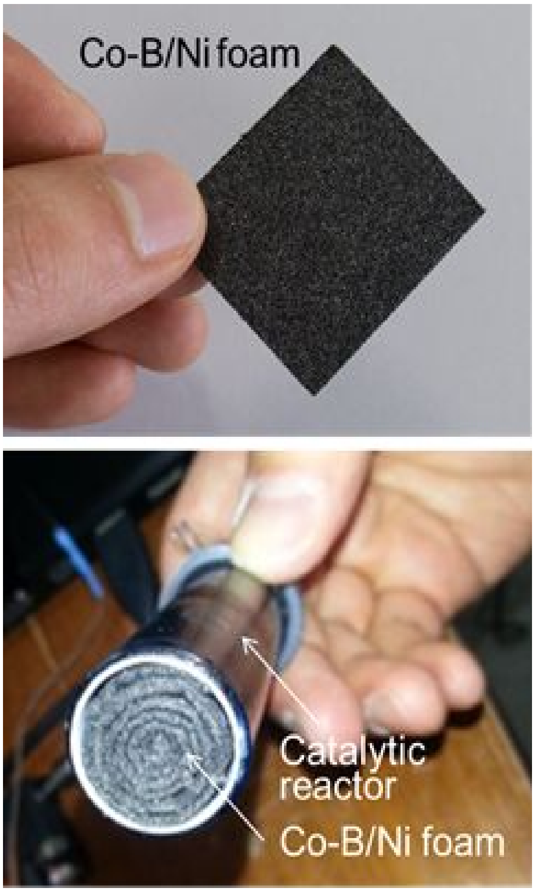

Fig. 5 Co-B/Ni foam catalyst for the $NaBH_4$ hydrolysis

C. Operating mechanism

The schematic of the control mechanism of the fuel cell system is shown in Fig. 6. Basically, all of driving parts including the pump, cooling fans, and purging valves, were controlled by the controller of the fuel cell system. The operating algorithm consists of three modes; the start-up, normal operation, and shutdown mode. First, when the system was initiated to be operated, the start-up mode was activated and the $NaBH_4$ solution that is stored in the fuel tank was supplied by the pump into the reactor. The fuel was injected continuously when the pressure in the reactor was lower than 3 Bar, while at the pressure higher than 3 bar, the fuel injection was stopped, going on to the normal operation mode.

The hydrogen generator was controlled according to the reactor pressure under the normal operation mode. At the pressure lower than 4 bar, the $NaBH_4$ solution was supplied by the pump, while the fuel supply stopped when the pressure reached 4 bar. On the other hand, when the pressure suddenly exceeded the safety limit, the hydrogen was discharged through the purging valve that is connected to the reactor. The safety limit was set to 5 bar in this case but it is changeable according to applications. If the reactor kept the pressure of 4 - 5 bar, the pump and purging valve were stopped and the reactor was ready to supply hydrogen to the fuel cell.

In the operation process of the hydrogen generator, the $NaBH_4$ solution was reacted on Co-B/Ni foam catalyst, generating hydrogen and $NaBO_2$. The $NaBO_2$ was discharged through the purging valve at an interval of the predetermined period according to the control algorithm. The generated hydrogen passed through the washing tank to remove sodium ions in hydrogen and was supplied to the fuel cell. When the fuel was exhausted or the system was terminated compulsorily, the shutdown mode was initiated; the fuel injection stopped and the catalyst was washed with the water in the washing tank that was pressurized by the hydrogen pressure.

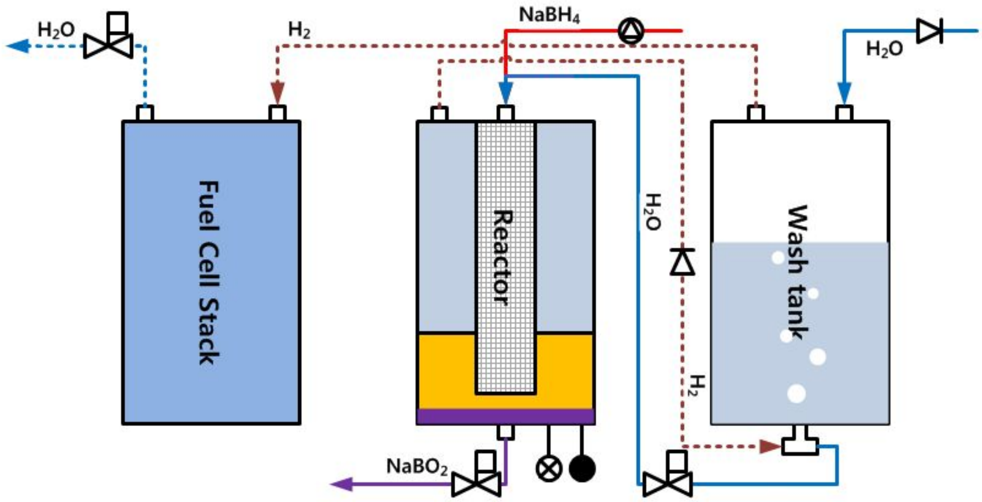

Fig. 6 Schematic of the control mechanism of the FC system

D. FC system performance and suitability evaluation

Figure 7 shows the experimental setup for evaluating the performance of the FC stack with a short circuit controller. We selected a 200 W_e FC stack featuring open-cathode and dead-ended anode operations to evaluate the FC controller. The oxidizer was supplied from ambient air using air-fans installed on the FC stack(open-cathode). The FC stack was pressurized by hydrogen gas(dead-ended anode), which was purged periodically to prevent water flooding. High-purity hydrogen was used without an additional humidifier for examining the effect of short-circuiting on the performance of the FC stack. The hydrogen pressure was regulated to 60kPa for all experiments. The hydrogen flow rate was measured using a flow meter(TSM-120) to calculate the amount of hydrogen consumed during the FC stack operation.

An electronic load (ESL-600) was used to obtain the I–V characteristics of the FC stack. The temperature, voltage, and current in the FC stack were recorded using a DAQ board (NI Corp.) and monitored via LabView software during the entire operation. Before evaluating the short circuit control, the cooling fans and purging valve controls were optimized to remove the heat generated by FC reaction and prevent water flooding, respectively. Two cooling fans were installed at the FC stack and the solenoid-type purging valve was connected to the end of its H_2-outport. The air flux of the cooling fans was 1.2773 m^3/min. The performance of the FC stack was evaluated at various conditions of (a) rpm of the cooling fans and (b) opening frequency of the purging value, and the results in the scenarios with and without the application of short circuit control were compared.

The suitability of the developed fuel cell system with chemical hydride hydrogen generator to the UAV applications was evaluated in the present study. First, the performance of hydrogen generator based on the selected catalyst was evaluated. Then, the possibility to be restarted after stopped for several hours was tested. In addition, the operation stability of hydrogen generator according to the reactor pressure was evaluated. The possibility of the stable hydrogen supply was examined by the long-term test. The hydrogen generator was integrated with the 100 W PEMFC stack and the power output was measured according to the electronic load. In addition, it was evaluated that the hydrogen generator stably supplied hydrogen to the fuel cell at various power demands. Finally, the hydrogen generator was compared with the compressed hydrogen that has high purity of 99.999% and was verified to be suitable as a hydrogen storage method for UAV applications.

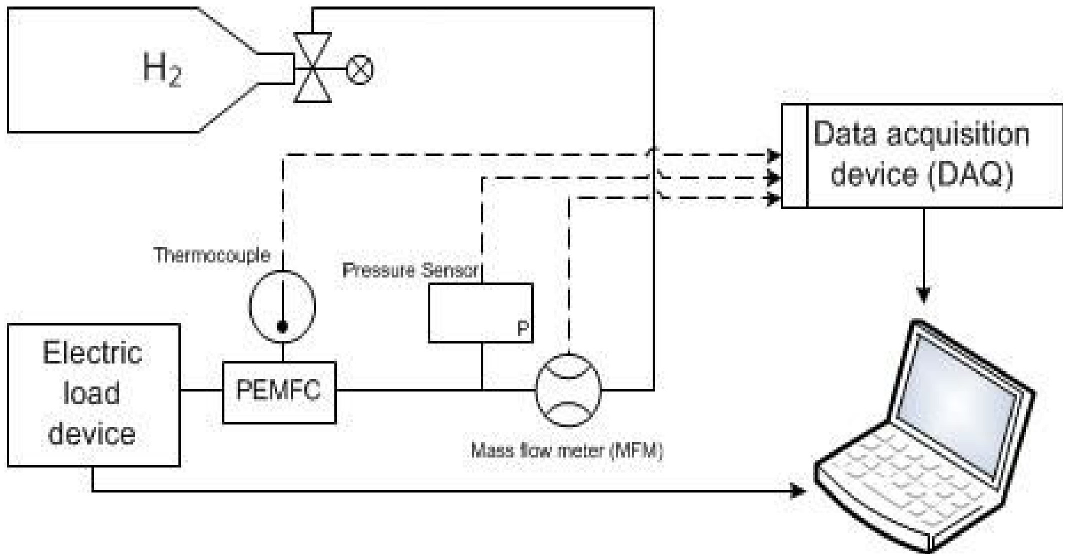

Fig. 7 Experimental setup for evaluating performance of FC stack sith short circuit controller

III. Results and discussion

A. Effect of controlling cooling fans and anode purging valve

Before applying humidification by short circuit control, the cooling fans and anode purging valve were optimized. Figure 8 shows the response characteristic of the FC stack according to the cooling fan control. The rotating speeds of the cooling fans were varied in the range of 10 – 80% of their maximum rpm, and the speed of response of the FC stack to the applied power load was different at different speeds of the cooling fans. At 10%, 30%, 50%, and 80% of the maximum rpm, the times taken by the FC stack to generate 70 W of power were observed to be 5.2, 3.3, 2.2, and 1.5 s, respectively, indicating that the response time reduced as the speed of the cooling fan increased, because more oxygen was supplied to the FC in proportion to the fan speed.

Figure 9 shows the voltage drop in the FC stack as a function of the purging period (25 – 100 s) at a load of 3 A. The FC stack was also evaluated at different purging durations in the range of 100 – 500 ms. Voltage drop refers to the difference between the voltages at the start and end of the purging period. Generally, the voltage in the FC stack decreases with time until the purging valve is reopened. At this point, the voltage is recovered, causing the spouting of water in the FC stack. As seen in Fig. 10, the voltage drop increased with increase in the purging period. For example, the voltage drops at purging periods of 25 and 100 s were 0.26 – 0.36 V and 1.19 – 1.60 V, respectively. In contrast, increase in the purging duration at a longer purging period reversed the voltage drop characteristics. When the purging period was fixed at 25 s, the voltage drops at purging durations of 100 and 500 ms were 0.26 and 0.36 V, respectively, indicating a slight increase in the voltage drop with increase in the purging duration.

However, for a purging period of 100 s, the voltage drop at purging durations of 100 and 500 ms were 1.60 and 1.19 V, respectively, indicating a decrease in the voltage drop.

The above results indicate that the voltage drop can be reduced by shortening the purging period or extending the purging duration at a longer purging period. This can be explained by the reaction of hydrogen with water inside the GDL. The water inside the FC stack was dispelled by the hydrogen pressure supplied when the purging valve was opened. In this situation, the inner condition of the FC stack is determined by the period and duration of the purging valve operation. At short purging periods, the hydrogen gas is purged before being consumed while passing through the GDL. Thus, the FC stack does not have sufficient time to react, causing its performance to degrade because hydrogen is frequently purged. Conversely, when the purging period is long enough to generate power smoothly, water flooding is caused, again resulting in performance degradation. One of the solutions to this problem is increasing the purging duration, as seen from the reduction in the voltage drop when the duration was increased from 100 to 500 ms at a purging period of 100 s.

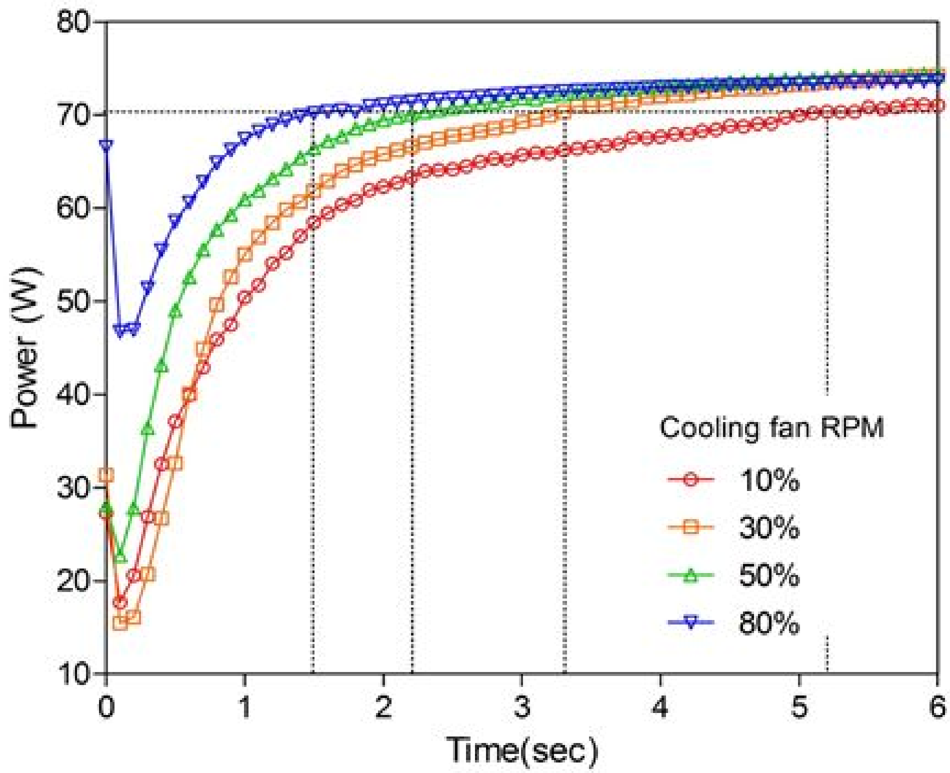

Fig. 8 Response characteristic of FC stack according to cooling fan control

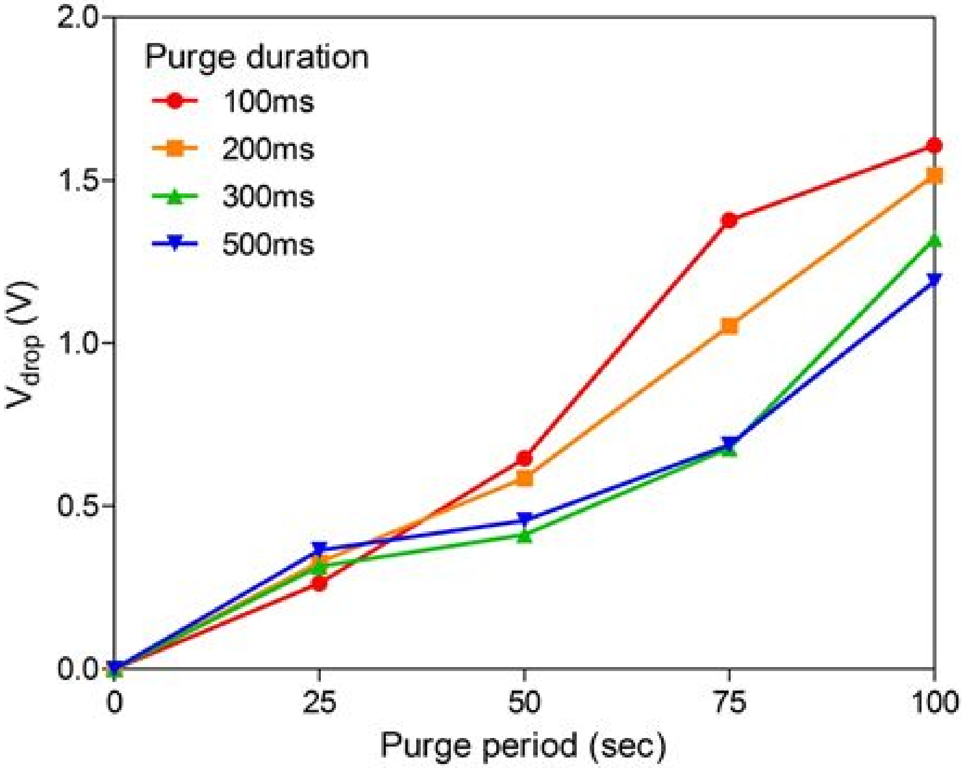

Fig. 9 Voltage drop in FC stack as function of purging period at 3A load

B. Performance improvement using short circuit technique

Figure 10 illustrates the improvement achieved in the FC stack performance using short circuit control. In this experiment, short circuit current was applied at 2 s to the FC stack, and its performance was compared to that without short circuit control. It was seen that performance was better at high load than at low load. At 3 A load, the power output of the FC stack with short circuit control (98 W) did not show a great improvement over that without (107 W), but at 9 A load, the improvement was much greater, with the output increasing from 218 to 252 W when short circuit control was applied, a 16% improvement over the performance without short circuit control.

Figure 11 shows the hydrogen flow rate upon operating the FC stack at 3 A load, during which hydrogen gas was purged at different periods of short-circuiting using the purging valve. Compared to operation without short circuit control, as much as 0.5 L/min more hydrogen was consumed during operation at 2 s. The measurement of hydrogen consumption across short circuit periods revealed 8.9% more consumption with short circuit control (3.54 L/min) than without (3.25 L/min). Furthermore, water was observed to be dispelled through the purging valve at high loads, indicating that sufficient water was generated using short circuit control.

Figure 12 shows the I–V performance curves for the short circuit periods of 2, 10, and 60 s. The open-circuit voltage (in the case without short circuit control) was lower (38.6 V) than those in the cases with short circuit control (> 42.0 V) because dry hydrogen gas was directly supplied in the former case, causing inadequate humidification in the FC stack. Thus, activation loss is expected to be greater when short circuit control is not applied. When loads were applied, the voltage decreased with increasing load, but the ohmic loss (a slope of the I-V curve) was slightly lower in cases with short circuit control than in those without. For example, for a load of 2–4 A, the ohmic loss was 0.90 Ω when short circuit control was applied at 2 s and 1.64 Ω without short circuit control, implying that the inner resistance of the FC stack was reduced by the water generated by short circuit control. At high loads (> 4 A), the effect of short circuit control increased with decrease in the period of short circuit. When a load of 8 A was applied, the power output at short circuit periods of 2, 10, and 60 s were 218.8, 225.9, and 232.3 W, respectively. Thus, the power output was seen to improve with a reduction in the short circuit frequency from the level without short circuit control (207.8 W).

Figure 13 shows hydrogen consumption as a function of current at different short circuit periods. At low loads (0 - 4 A), hydrogen consumption increased with an increase in the short circuit period. At loads of 0 - 2 A, hydrogen consumption doubled (0.49 - 1.09 L/min) at a short circuit interval of 2 s from that when no short circuit control was applied, whereas at high loads (> 6 A), it was nearly the same regardless of short circuit control, except when applied at 2 s. At a load of 8 A, 3.26 L/min of hydrogen was consumed without short circuit control, and during short-circuiting at 10 and 60 s, 3.26 and 3.24 L/min were consumed, respectively, which are almost equal to the case without short circuit control. However, hydrogen consumption was slightly higher at a short circuit period of 2 s, implying that a very small short circuit interval results in excessive hydrogen consumption, although it improves the performance of the FC stack.

At high current loads, hydrogen consumption was similar in cases with and without short circuit control. Thus, at low loads, short circuit control should be applied in long intervals or not at all, because the improvement in performance relative to hydrogen consumption is not significant over different short circuit periods. In contrast, at high loads, the short circuit period should be reduced to maximize the power output even if it results in greater hydrogen consumption.

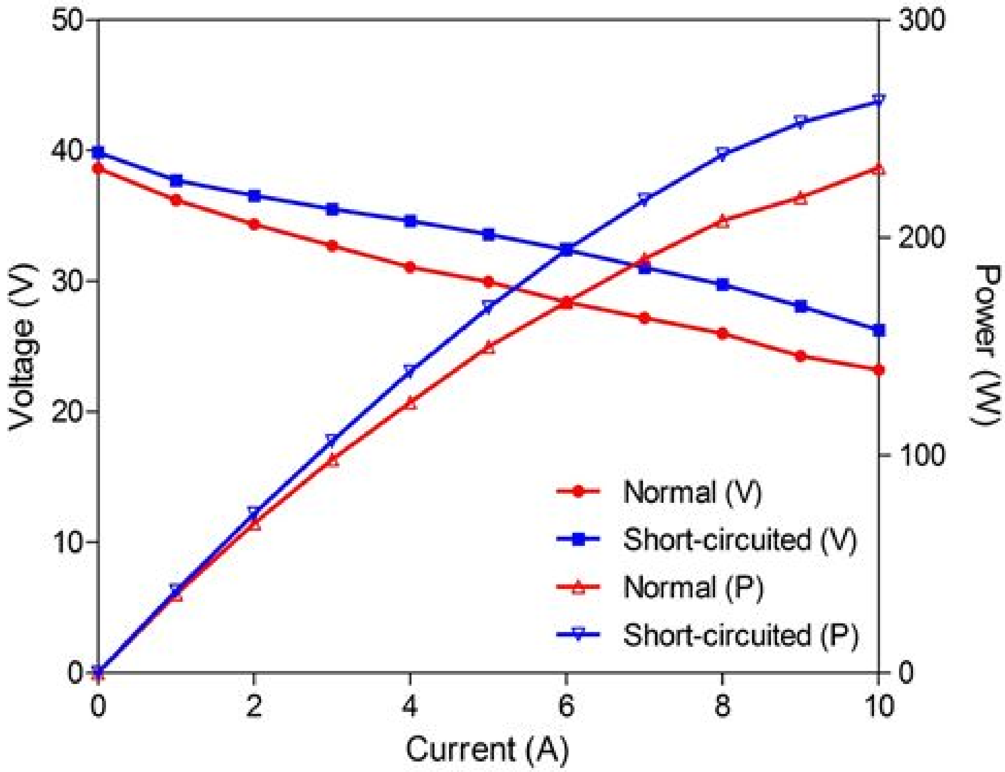

Fig. 10 Improvement in FC stack performance using short circuit control

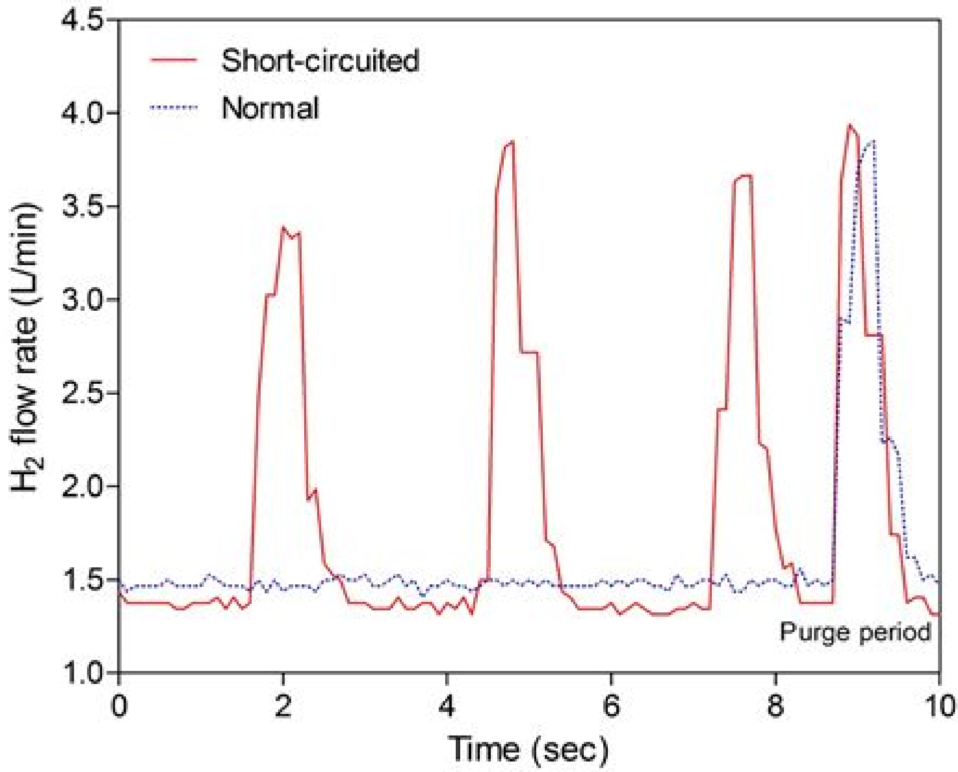

Fig. 11 Hydrogen consumption in FC stack with and without short circuit at 3A load

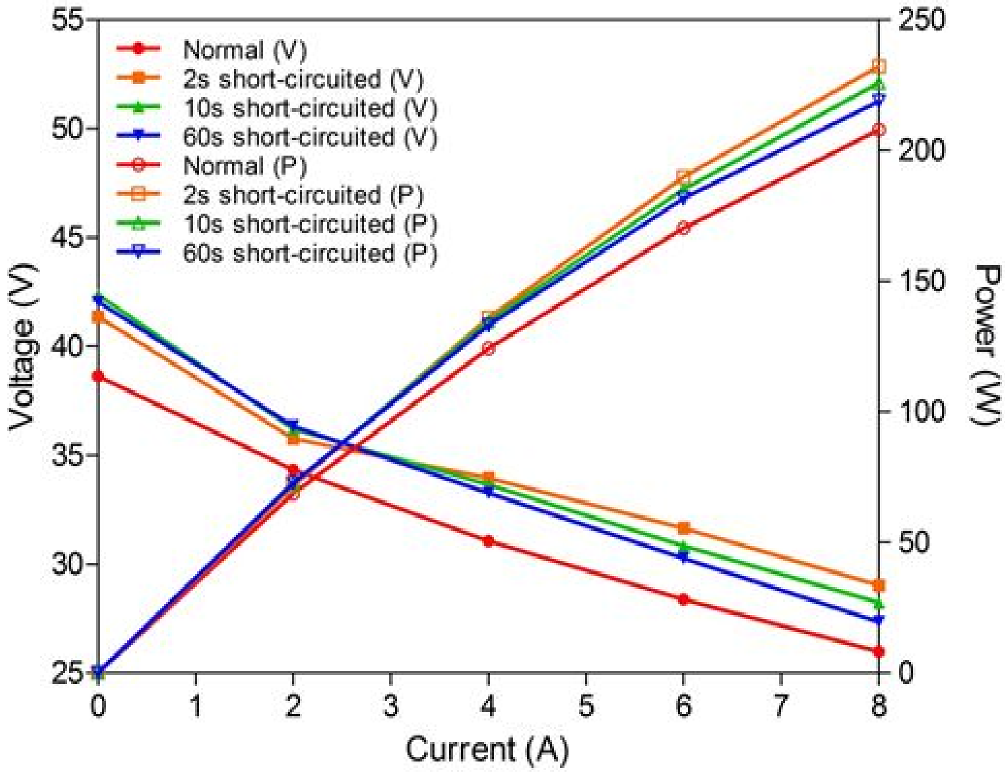

Fig. 12 I-V performance curves for different short circuit periods

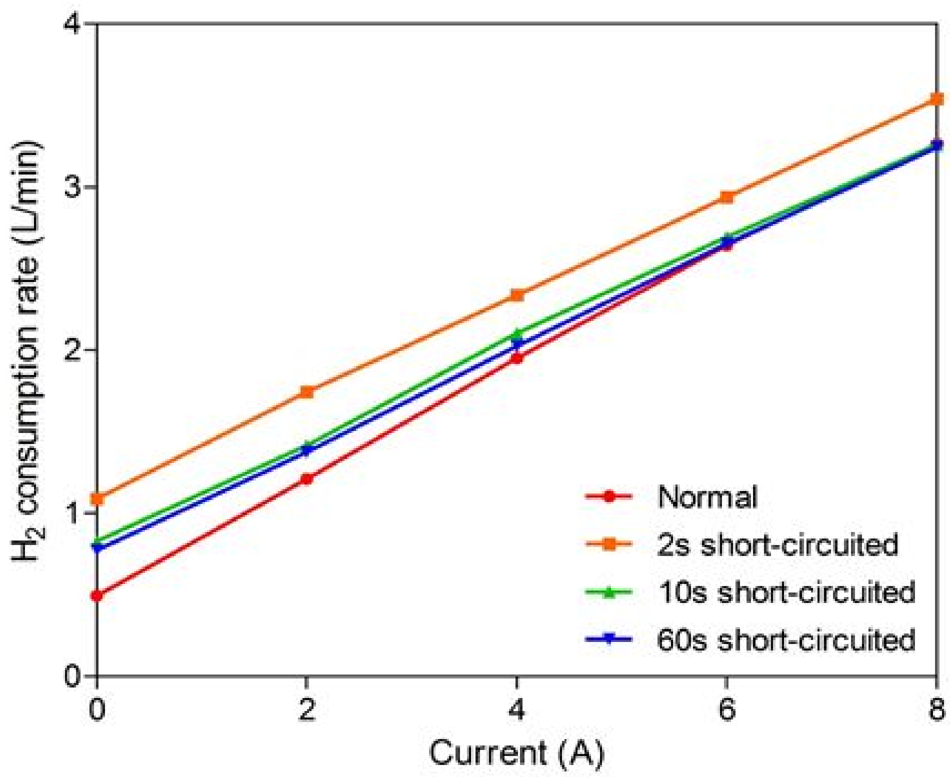

Fig. 13 Hydrogen consumption as function of current at different short circuit periods

C. Performance of hydrogen generator

The experimental result on reactivity and reusability of the used catalyst is shown in Fig. 14. The 15 wt.% $NaBH_4$ solution of 80 mL was injected for 400 seconds and then after washing the catalyst it remained as it is for 1 hour. Next, the system was restarted and the performance of hydrogen generation between the first and the second time was compared. The start-up time for the pressure to reach 3 bar at the second time became longer than that at the first time. However, the reactor pressure stably maintained 4 bar at the normal operation mode. The fuel was injected again to the reactor when the reactor pressure decreased down to 4 bar. The $NaBH_4$ solution of 0.13 mL was injected when the pump was operated once for 50 milliseconds. If the operating time at the pressure lower than 4 bar became long, the number of the fuel injection also increased to recover the pressure. If the pressure was higher than 5 bar, hydrogen was discharged through the purging valve. Therefore, the reactor maintained the pressure range of 4 - 5 bar.

The frequency of the fuel injection and the borate purging to recover the pressure in the reactor is shown in Fig. 15. The duration when the pressure kept lower than 4 bar became long from (a) to (d). The number of the fuel injection increased with increasing the duration to recover the pressure in the reactor. When the pressure exceeded 5 bar due to the excessive fuel supply, the number of the borate purging also increased to maintain the pressure to be lower than 5 bar as the number of the fuel injection increased from (a) to (d). Although the pressure varied sharply, it could be controlled within the determined range by controlling the operation frequency of the pump and the valve.

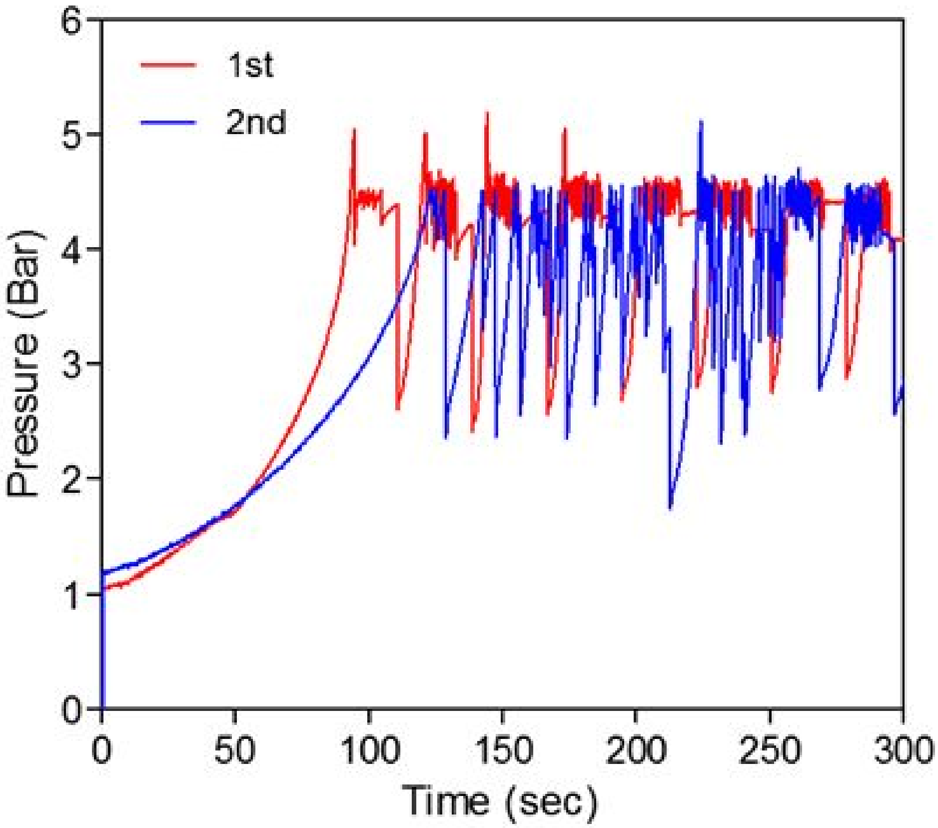

Fig. 14 Reactivity and reusability of the prepared catalyst

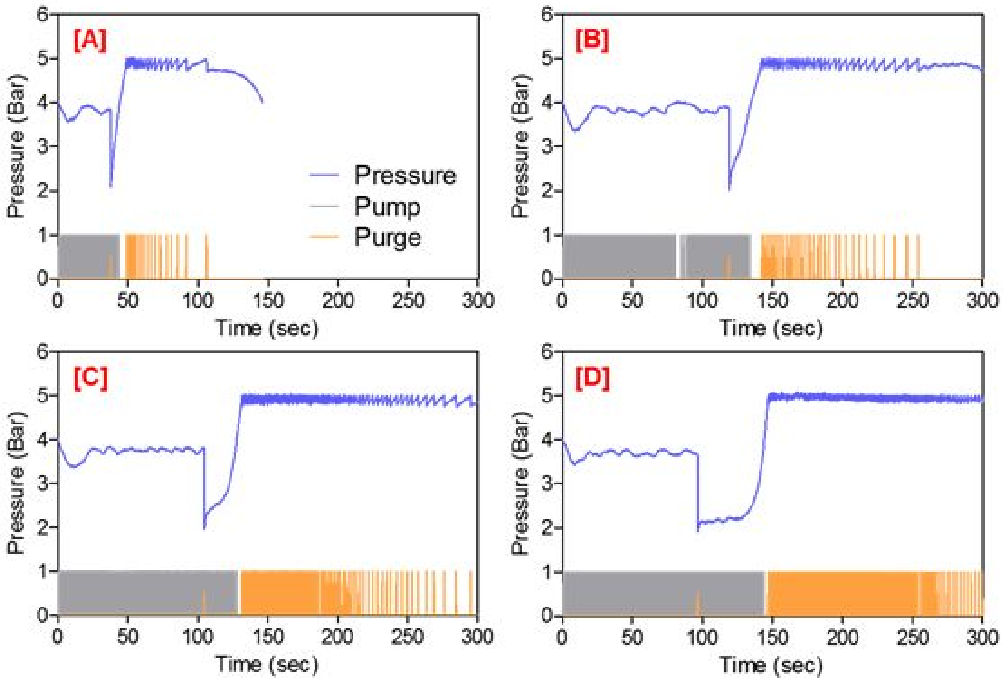

Fig. 15 Frequency of the fuel injection and the borate purging to recover the pressure in the reactor. The duration when the pressure kept lower than 4 bar became long from (a) to (d)

D. Operating characteristics during the long-term test

Operating characteristics of the hydrogen generator during the long-term test at the different hydrogen supply rate is shown in Fig. 16. The results were divided into the section (a) and (b) according to the hydrogen supply rate of 1.2 L/min and 1.7 L/min, respectively. The hydrogen generated in the reactor was discharged at the controlled flow rate through the regulator and orifice. Looking at the start-up time of the section (a), the response time was required to fill the reactor with hydrogen until the pressure reached 3 bar. After the start-up time passed, the system mode changed from the start-up to the normal operation mode. For the start-up time, the fuel more than desired was supplied, which caused the reactor to be over-pressurized into the pressure higher than 5 bar at 50 seconds in Fig. 15(a). Immediately, the pressure was controlled to 5 bar through the purging valve, resulting that the hydrogen supply rate was maintained to 1.2 L/min. In addition, the reactor temperature increased by 90°C due to the heat of reaction of the excessive fuel with the catalyst.

After the system was stopped for 30 minutes, the hydrogen supply rate increased to 1.7 L/min at the section (b). Thus, the pressure in the reactor was dropped more sharply because hydrogen more than the section (a) was discharged. Thus, the number of the fuel injection increased more compared to the section (a) and the purging valve was also opened more frequently. The reactor maintained the temperature near to 70°C which was relatively low compared to the section (a). The cooling fans of the reactor were fully operated due to the rapid rise of temperature and the $NaBO_2$ under the elevated temperature was discharged more frequently through the purging valve. Thus, the temperature at the section (b) was lower than that at the section (a). Although the reactor was operated for a long time, the temperature was maintained to be suitable to sustain the hydrolysis of $NaBH_4$ and to prevent the fuel from evaporating that caused hydrogen contaminated. In addition, it can be seen that the hydrogen generation was stable when the required hydrogen supply rate changed during the operation.

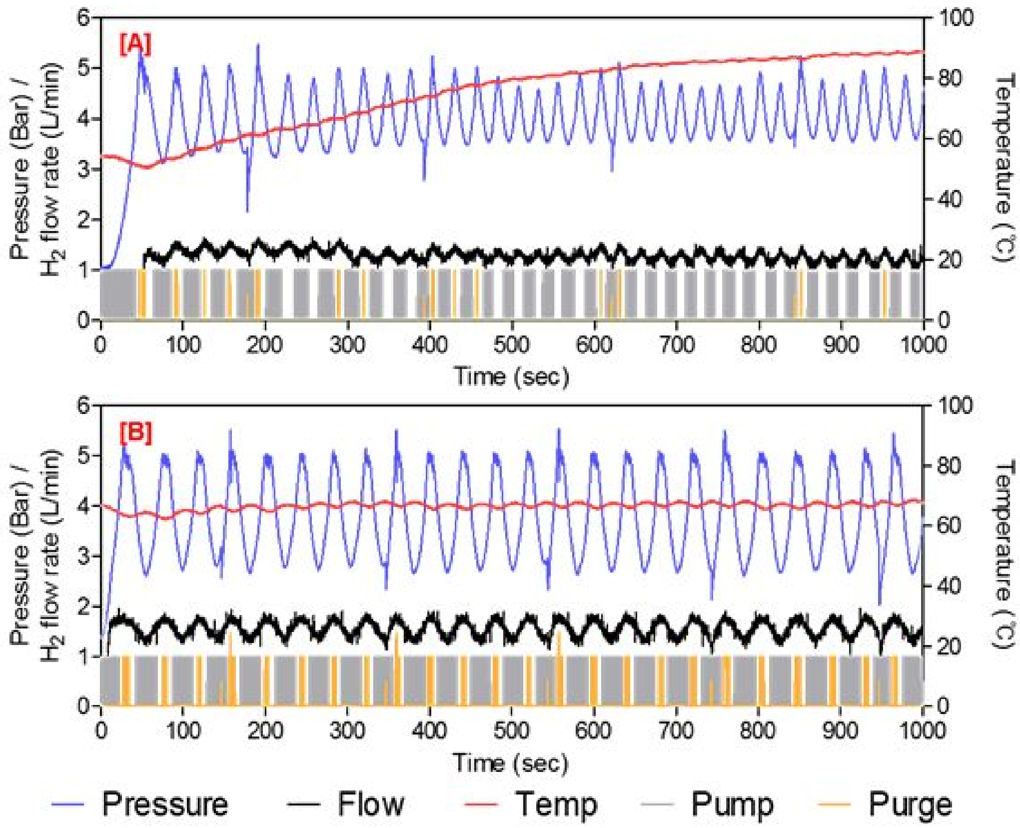

Fig. 16 Operating characteristics of the hydrogen generator during the long-term test at the different hydrogen supply rate: (a) 1.3 L/min and (b) 1.7 L/min

E. Integrated performance with 100 W PEMFC

The performance of the PEMFC operated by the hydrogen generator is shown in Fig. 17. The output power of the PEMFC as the electronic load increased is shown in Fig. 17 (a). The reactor pressure and hydrogen supply rate during the PEMFC operation is shown in Fig. 17 (b). The electronic load was increased sequentially from 0 to 100 W and maintained 100 W after 180 seconds. Periodic peaks of hydrogen supply rate were observed, which was to prevent the fuel cell from water flooding by operating the purging valve that is connected to the hydrogen venting port. The fuel injection frequency increased as increasing the electronic load because the required hydrogen supply rate also increased. The PEMFC consumed approximately 1.2 L/min of hydrogen to generate the electric power of 100 W. As the increase of the electronic load, the hydrogen supply rate increased and thus the hydrogen pressure in the reactor was dropped sharply. Therefore, the fuel injection frequency also increased. The purging valve was open more frequently according to the rapid rise of the pressure and then the borate was discharged. The minimum operating pressure was dropped from 3.0 bar to 2.75 bar as the increase of the electronic load except for the pressure drop caused by opening the purging valve for the $NaBO_2$ disposal. That was because the hydrogen supply rate increased, however, the reactor was still buffering the rapid consumption of hydrogen according to the electronic load. Therefore, the system was operated stably according to the electronic load.

Compressed hydrogen with a high purity of 99.999% was used for comparison with the hydrogen generator. The performance of PEMFC was measured using the hydrogen generator and the compressed hydrogen, respectively. The performance comparison of the hydrogen generator with the pure hydrogen is shown in Fig. 18. It can be seen that there were no considerable differences in voltage and output power between two cases. Form the result, it was verified that the PEMFC system using the chemical hydride-based hydrogen generator makes it possible that the stable hydrogen supply for the fuel cell-powered UAV.

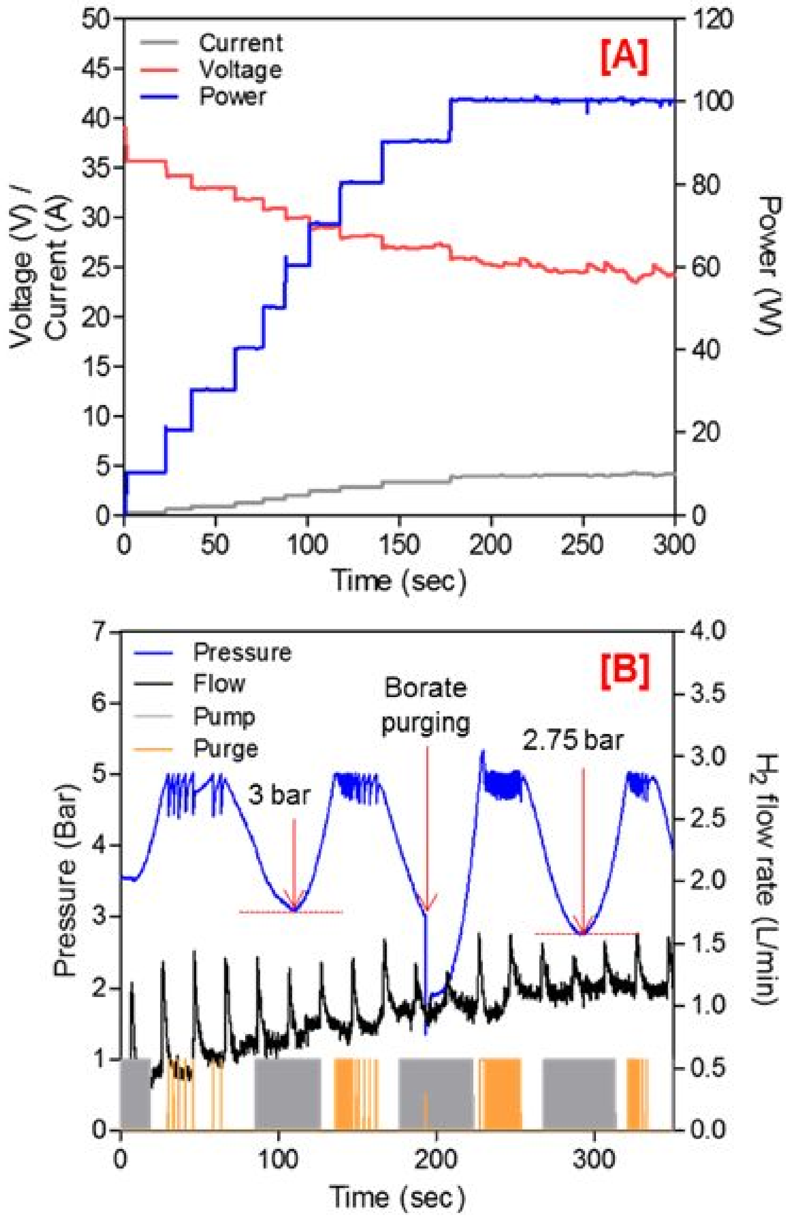

Fig. 17 Performance of the PEMFC system using the hydrogen generator: (a) the output power of the PEMFC as the electronic load increased and (b) the reactor pressure and hydrogen supply rate during the fuel cell operation

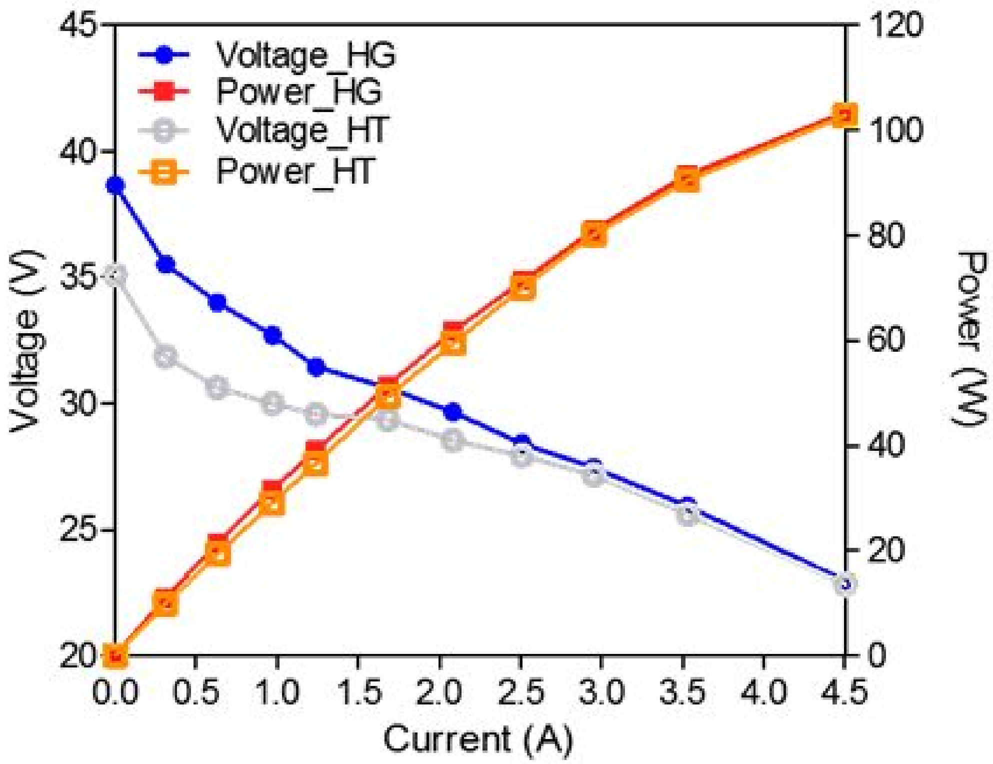

Fig. 18 Performance comparison of the hydrogen generator with the pure hydrogen

IV. Conclusion

In this study, fuel cell system for UAVs are designed. First, the PEMFC stack was short-circuited to humidify the electrolyte membrane and improve power output for UAV applications. A PEMFC of dead-ended anode/open-cathode type with dry hydrogen and not humidified externally was used. A short circuit controller using a power-MOSFET was developed for the experiment. From the results, the following conclusions were drawn:

1) Voltage drop varied with the control of the purging valve. At short purge periods (0 - 25 s), the voltage drop reduced as the purge duration decreased. On the contrary, at long purge periods (75 - 100 s), it reduced with increase in the duration.

2) Power output was improved by short-circuiting the FC. At low loads (0 - 3 A), the improvement in the power output was not significant but at high loads (7 - 10 A), it was quite noticeable, demonstrating a 16% increase from that at no load or no short circuit.

3) When the FC was short-circuited, hydrogen consumption doubled at low loads (0 - 2 A) but remained approximately the same as when the FC was not short-circuited at high loads (6 - 8 A).

4) FC performance was improved further by reducing the short circuit period. When the FC was short-circuited at 2 s, hydrogen consumption was 8% more but the power output increased by 16% at a load of 8 A. To enhance the power output without using a short circuit controller, more FCs must be stacked, making the FC system heavy, bulky, and thereby unsuitable for UAV applications. Therefore, using a short circuit controller increases the specific power density of the FC stack and results in a compact FC system.

And second, the compact PEMFC system using the chemical hydride as a hydrogen source was developed. The fuel cell system consists of three parts; PEMFC stack, hydrogen generator, and fuel tank. The hydrogen generator had an all-in-one reactor in which the $NaBH_4$ hydrolysis took place and the generated hydrogen was stored temporally. The $NaBH_4$ solution was stored in the fuel tank that is easy to be detachable from the system, which facilitates the safe storage and porterage. The performance of the hydrogen generator was evaluated at various operation conditions. The $NaBH_4$ solution was injected into the reactor when the reactor pressure was less than 4 bar. On the other hand, when the pressure was higher than 5 bar, hydrogen was discharged through the purging valve. Therefore, the reactor maintained the pressure range of 4-5 bar. The fuel injection frequency and hydrogen supply rate increased as increasing the electronic load. The PEMFC consumed approximately 1.2 L/min of hydrogen to generate the electric power of 100 W. As the increase of the electronic load, the hydrogen supply rate increased and thus the reactor pressure was dropped sharply. Therefore, the fuel injection frequency also increased. The purging valve was operated more frequently according to the rapid increase of the pressure. Based on this control mechanism, the hydrogen supply to the fuel cell was stabilized to be suitable for UAV applications.

References

[1] http://www.avinc.com/uas/stratospheric/global_observer/

[2] http://www.naval-technology.com/projects/ion-tiger-uav/

[3] http://www.wpafb.af.mil/news/story_print.asp?id=123081119

[4] http://www.boeing.com/boeing/bds/phantom_works/phantom_eye.page

[5] http://www.smartfish.ch/index.cfm/fuseaction/show/path/1-129.htm

[6] http://www.energyor.com/energyor/news.cfm

[7] http://www.iai.co.il/2013/35099-39739-en/IAI.aspx

[8] http://news.wsu.edu/2013/06/17/unique-unmanned-aerial-vehicle-takes-flight/#.Unhng_l7K3w

[9] http://english.web.ncku.edu.tw/files/16-1005-66154.php

[10] http://erian.ntu.edu.sg/ResearchAreas/Pages/FuelCells.aspx

[11] Kim T, Kwon S. Design and development of a fuel cell-powered small unmanned aircraft. Int J Hydrogen Energy 2012; 37:615-22.

[12] Kim T. Fully integrated micro PEM fuel cell system with $NaBH_4$ hydrogen generator. Int J Hydrogen Energy 2012;37:2440-6.

[13] Larminie J, Dicks A. Fuel Cell Systems Explained. 2nd ed. West Sussex: John Wiley and Sons; 2003.

[14] Owejan J P., Gagliardo J J., Sergi J M., Kandikar S G., Trabold T A.. Water management studies in PEM fuel cells, Part I: Fuel cell design and in situ water distributions. Int J Hydrogen Energy 2009; 34:3436-44.

[15] Zhan Z, Wang C, Fu W, Pan M. Visualization of water transport in a transparent PEMFC. Int J Hydrogen Energy 2012; 37:1094-105.

[16] Choi JW, Hwang Y, Seo J, Lee DH, Cha SW, Kim MS. An experimental study on the purge characteristics of the cathodic dead-end mode PEMFC for the submarine or aerospace applications and performance improvement with the pulsation effects. Int J Hydrogen Energy 2010; 35:3698-711.

[17] Hwang Y, Lee D, Choi JW, Kim S, Cho SH, Park J, Kim MS, Jang JH, Kim SH, Cha S. Enhanced diffusion in polymer electrolyte membrane fuel cells usin

g oscillating flow. Int J Hydrogen Energy 2010; 35:3676-83.

[18] Choi JW, Hwang Y, Cha SW, Kim MS. Experimental study on enhancing the fuel efficiency of an anodic dead-end mode polymer electrolyte membrane fuel cell by oscillating the hydrogen. Int J Hydrogen Energy 2010; 35:12469-79.

[19] Sean S. Muir, Xiangdong Yao. Progress in sodium borohydride systems as a hydrogen storage material: Development of hydrolysis catalysts and reaction. Int J Hydrogen Energy 2011; 36:5983-97

[20] Hyun Tae Hwang, Arvind Varma. Hydrogen storage for fuel cell vehicles Chemical Engineering. 2014; 5:42-8

[21] SeungJae Yang, Haesol Jung, Taehoon Kim, ChongRae Park. Recent advances in hydrogen storage technologies based on nanoporous carbon materials. Progress in Natural Science: Materials International 2012; 22:631-8

[22]S.U. Jeong, R.K. Kim, E.A. Chob, H.-J. Kim, S.-W. Nam, I.-H. Oh, S.-A. Hong, S.H. Kim. A study on hydrogen generation from $NaBH_4$ solution using the high-performance Co-B catalyst. J of Power Sources 2005; 144:129-34

[23] Rajasree Retnamma, Augusto Q. Novais, C.M. Rangel. Kinetics of hydrolysis of sodium borohydride for hydrogen production in fuel cell applications: A review. Int J Hydrogen Energy 2011; 36:9772-90

[24] N. Patel, R. Fernandes, A. Miotello. Promoting effect of transition metal-doped Co–B alloy catalysts for hydrogen production by hydrolysis of alkaline $NaBH_4$ solution. J of Catalysis 2010; 271:315-24

[25] R. Fernandes, N. Patel, A. Miotello. Hydrogen generation by hydrolysis of alkaline $NaBH_4$ solution with Cr-promoted Co–B amorphous catalyst. Applied Catalysis B: Environmental 2009; 92:68-74

[26] Hongjing Tian, Qingjie Guo, Dongyan Xu. Hydrogen generation from catalytic hydrolysis of alkaline sodium borohydride solution using at tapulgite clay-supported Co-B catalyst. J of Power Sources 2010; 195:2136-42

[27] T. Vilarinho-Franco, R. Tenub, J. Delmas, M. Heitzmann, P. Capron, C. Goutaudier. Lifetime analysis of a hydrogen generator by hydrolysis of sodium borohydride. Energy Procedia 2013; 36:1192-201

[28] Jaeyoung Lee, Kyung Yong Kong, Chang Ryul Jung, Eunae Cho, Sung Pil Yoon, Jonghee Han, Tai-Gyu Lee, Suk Woo Nam. A structured Co–B catalyst for hydrogen extraction from $NaBH_4$ solution. Catalysis today 2007; 120:305-10
[29] T. Sousa, V.R.Fernandes, P.J.R.Pinto, Y.Slavkov, L.Bosukov, C.M.Rangel. A sodium borohydride hydrogen generation reactor for stationary applications: Experimental and reactor simulation studies. Chemical Engineering Science 2012; 84:70-9
[30] Wei Ye, Huamin Zhang, Dongyan Xu, Li Maa, Baolian Yi. Hydrogen generation utilizing alkaline sodium borohydride solution and supported cobalt catalyst. J of Power Sources 2007; 164: 544-8
[31] S. Galli, M. De Francesco, G. Monteleone, R. Oronzio, A. Pozio. Development of a compact hydrogen generator from sodium borohydride. Int J Hydrogen Energy 2010; 35:7344-9
[32] Steven G. Chalk, James F. Miller. Key challenges and recent progress in batteries, fuel cells, and hydrogen storage for clean energy systems. J of Power Sources 2006; 159:73-80
[33] Li Zhou. Progress and problems in hydrogen storage methods. Renewable & Sustainable Energy Reviews 2005; 9:395-408
[34] Ping Chen, Min Zhu. Recent progress in hydrogen storage. Materials today 2008; 11:36-43
[35] D.J. Durbin, C. Malardier-Jugroot. Review of hydrogen storage techniques for on board vehicle applications. Int J Hydrogen Energy 2013; 38:14595-14617
[36] Scott W. Jorgensen. Hydrogen storage tanks for vehicles: Recent progress and current status. Current Opinion in Solid State and Materials Science 2011; 15:39-43
[37] Bin Hong Liu, Qian Li. A highly active Co-B catalyst for hydrogen generation from sodium borohydride hydrolysis. Int J Hydrogen Energy 2008; 33:7385-91
[38] B.H. Liu, Z.P. Li, L.L. Chen. Alkaline sodium borohydride gel as a hydrogen source for PEMFC or an energy carrier for $NaBH_4$-air battery. J of Power Sources 2008; 180:530-4

[39] A.M.F.R. Pinto, D.S. Falcão, R.A. Silva, C.M. Rangel. Hydrogen generation and storage from hydrolysis of sodium borohydride in batch reactors. Int J Hydrogen Energy 2006; 31:1341-7

[40] Valentina G. Minkina, Stanislav I. Shabunya, Vladimir I. Kalinin, Vladimir V. Martynenko, Alevtina L. Smirnova. Stability of alkaline aqueous solutions of sodium borohydride. Int J Hydrogen Energy 2012: 37:3313-8

이력서

성　　명 : 김진철

생년월일 : 1988년 1월 5일

출 생 지 : 경상북도

본　　적 : 경상북도 칠곡군 약목면 덕산2길 14

학력

2006.3. ~ 2013.2. : 조선대학교 항공우주공학과 (B.S.)

2013.3. ~ 2015.2. : 조선대학교 항공우주공학과 (M.S.)

RESEARCH ACHIEVEMENTS

INTERNATIONAL JOURNALS

1. Jincheol Kim, Taegyu Kim, "Humidification of PEM Fuel Cell using a Short-Circuit Control for UAV applications," International Journal of Hydrogen Energy, 39, 7925-7930, 2014

INTERNATIONAL CONFERENCES

1. Jincheol Kim, Taegyu Kim "Compact PEM fuel cell system using chemical hydride hydrogen source for portable power generators," *Proceedings of The 6th International Conference on Applied Energy*, 2014.5.30.-6.2, Taipei, Taiwan.
2. Taegyu Kim, Jincheol Kim, Ju-hyeong Sim, Shinuang Kang, "Chemical Hydride-based PEM Fuel Cell System for Real World Commercial Applications," *Proceedings of the 20th World Hydrogen Energy Conference*, 2014.6.16.-6.19 Gwangju, Korea.

DOMESTIC CONFERENCES

1. Jincheol Kim, Taegyu Kim, "Design of N_2O Monopropellant Thruster System," Proceedings of KASA Annul Fall Meeting, 2011.11.9-11.11, Yongpyong, Korea.
2. Jincheol Kim, Sung Uk Kim, Dong Min Kim, Taegyu Kim, "Study on Polymer Electrolyte Membrane Fuel Cell for UAV Applications," *Proceedings of KSPE Annual Spring Meeting*, 2012.5.17.-5.18, Gumi, Korea.

3. Jincheol Kim, Taegyu Kim, "Study on Improvement of Ionic Conductivity of Fuel Cell Electrolyte Membrane using Electrical Overcurrent," *Proceedings of KICHE Annul Fall Meeting*, 2013.4.24-4.26, Gwangju, Korea.
4. Jincheol Kim, Taegyu Kim, "Design on Humidification Controller of Hydrogen Fuel Cell for Aircraft Applications," *Proceedings of SASE Spring Conference*, 2013. 5.9-5.10, Muju, Korea.
5. Taegyu Kim, Ju-hyeong Sim, "Development of Chemical Hydride-based 200W Fuel Cell System for Electric UAVs," *Proceedings of KSPE Annual Fall Meeting*, 2013.12.5.-12.6, Kyungju, Korea.
6. Jincheol Kim, Taegyu Kim, Changwook Lee, Jip Kim, "Design and performance evaluation of overcurrent generator for internal humidification of polymer electrolyte membrane fuel cell," *Proceedings of KSME conference*, 2013.12.18.-12.20, Jeongseon, Korea.
7. Jincheol Kim, Taegyu Kim, "Design of a chemical hydride-based compact PEMFC system as a main power source for UAVs," *Proceedings of SASE Spring Conference*, 2014. 5.14-5.16, Jeju, Korea.
8. Jincheol Kim, Taegyu Kim, "Design of Fuel Cell System based on Chemical hydride for SUAVs," *proceedings of SASE Fall Conference,* 2014. 10.29-10.31, Muju, Korea